

# MAGNETOTELLURIC INVERSION FOR CHARACTERISATION OF COMPLEX AQUIFER SYSTEMS

**Ralf Schaa\***

Lecturer  
Curtin University  
Exploration Geophysics  
ralf.schaa@curtin.edu.au

**Brett Harris**

Associate Professor  
Curtin University  
Exploration Geophysics  
brett.harris@curtin.edu.au

**Andrew Pethick**

Lecturer  
Curtin University  
Exploration Geophysics  
andrew.pethick@curtin.edu.au

**Alex Costall**

PhD Candidate  
Curtin University  
Exploration Geophysics  
alex.costall@postgrad.curtin.edu.au

**Jon-Philippe Pigois**

Department of Water and Environmental Regulation  
Western Australian Government  
jon-philippe.pigois@dwer.wa.gov.au

**Eric Takam Takougang**

The Petroleum Institute  
etakougang@pi.ac.ae

*\*presenting author asterisked*

## SUMMARY

Data from a magnetotelluric survey along a 2D transect across the basin-scale Badaminna Fault zone in the northern Central Perth Basin was used to augment the information from a limited number of monitoring wells across the fault zone. The magnetotelluric method was employed to provide continuous spatial information of the subsurface electrical resistivity for hydrogeological interpretation from the near surface to depths exceeding 2 km, where hydrostratigraphic units are offset by vertical fault displacement. Unconstrained 2D inversion resulted in a somewhat compartmentalized subsurface structure consistent with the known shallow hydrostratigraphy from borehole information, seismic and airborne EM. At larger depths broad conductive structures can be linked to increasing salinities.

**Key words:** Magnetotelluric, 2D Inversion, Hydrogeophysics, Faults

## INTRODUCTION

The hydrogeology of the (onshore) Perth Basin consist of a multi-layered system of heterogeneous sedimentary aquifers supplying 46% of potable water for the Perth metropolitan area (7% from dams and 47% from desalinated water) (Water Corporation, 2016). The Perth Basin is separated by the north-trending Darling Fault from the Archean Yilgarn Craton in the east and extends ~1000 km along the western margin of Australia, where it thins towards oceanic crust in deep water about 100 km offshore (Crostella & Backhouse, 2000, p. 1). In the Perth region the Gngangara groundwater system along the coastal plain north of the Swan River provides most of the groundwater resources for Perth. This system consist of four major aquifers: 1) the shallow, unconfined Superficial aquifer, 2) the shallow, semi-confined Mirrabooka aquifer, 3) the deep, partially-confined Leederville aquifer and 4) the deep, mostly confined Yarragadee aquifer (Department of Water [DoW], 2017).

The Perth region is dependent on deeper groundwater resources from both Leederville and Yarragadee aquifers to reduce the effect of groundwater abstraction on the Superficial aquifer (DoW, 2016), and groundwater management becomes increasingly important to mitigate increased water usage due to urbanisation and effects of climate change (Barron et al., 2014). Ongoing characterisation of geological structures and their influence on groundwater resources is therefore central to refine predictive groundwater modelling of the Gngangara aquifer system.

In this context, a pilot magnetotelluric survey was carried out to investigate the electrical resistivity across the Badaminna Fault zone from the near-surface to depths exceeding 2 km. Fault offset resulted here in the juxtaposition of stratigraphic units with contrasting hydrologic properties that is considered to impact groundwater flow. The distribution of subsurface electrical resistivity can provide further structural information across the fault zone at larger depths away from boreholes, for example, clays and shales (aquicludes) can be differentiated from sands and sediments (aquifers), and may indicate zones of fluid flow across the fault, potentially providing clues of aquifer connectivity across the fault; and furthermore, the MT-derived resistivities may indicate zones of different salinities across the Badaminna Fault zone and at depth.

The north-trending Badaminna fault zone is a basin-scale extensional fault system, running mainly offshore in the central Perth Basin of Western Australia (Figure 1). Displacement along the Badaminna Fault system observed in seismic transects across the onshore portion of the fault, has resulted in vertical offsets of the aquifer systems in the Central Perth Basin (Figure 2A). In addition, borehole data showed that the Badaminna Fault separates here aquifer systems of different salinity and age, and fault offset disconnected western and eastern portions of the Leederville aquifer while connecting the Leederville with the Yarragadee aquifer over a thickness of up to 500 m (Leyland, 2012, p.48; DoW, 2016). The pilot MT survey was carried out to attempt further spatial characterisation of the displaced aquifer systems across the Badaminna Fault zone.

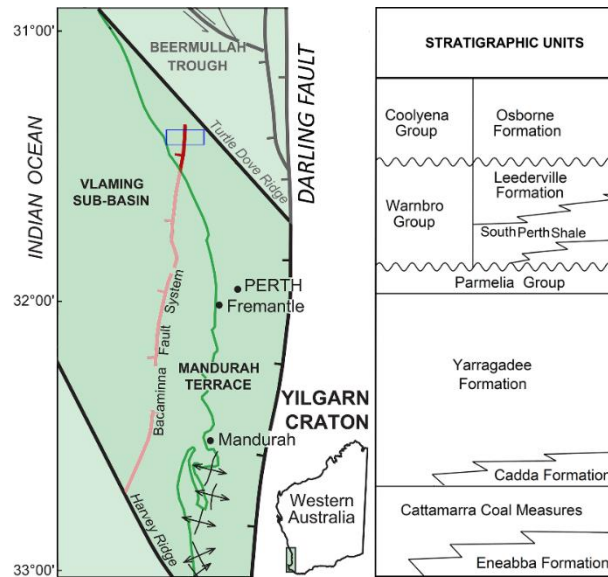


Figure 1 Basin subdivisions of the central Perth Basin, with the onshore portion of the Badaminna Fault (BF) highlighted in darkred. The blue box shows the region of the MT survey. Also shown is the simplified stratigraphy of the area (modified after Crostella & Backhouse, 2000, p. 2 & p.3).

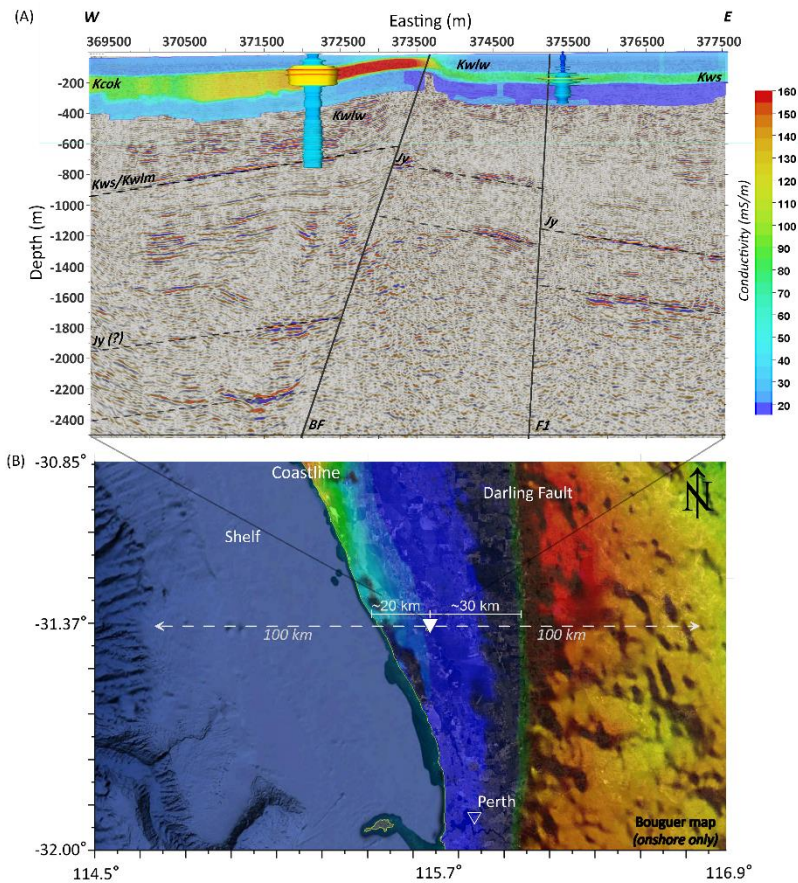


Figure 2 (A): Airborne EM conductivity cross-section along the MT survey line superimposed on a coincident seismic line, serving as a starting model for MT inversion. The Badaminna Fault (BF) separates the western and eastern stratal packages, connecting the Wanneroo and Yarragadee aquifer. Elevated AEM conductivities in green/red colours show the shallow layers of the Kardinya Shale (Kcok) in the west and the South Perth Shale (Kws) on the east, respectively. Some identified horizons from the seismic are indicated by their abbreviations: Kwlw: Wanneroo Mb – Kwlm: Marigniuup Mb – Jy: Yarragadee Fm. Underlying the Yarragadee Fm are the Cadda Fm and Cattamarra Coal Measures, which can be broadly identified on the seismic section. (B): Map of Perth Basin with onshore Bouguer gravity overlain, showing the Darling Fault anomaly in the east and the low Bouguer values of the sedimentary central Perth Basin. The MT survey location is indicated by the triangle. The offshore part of the basin shows the continental shelf, about 100 km offshore to the edge of continental crust in water depths of up to 4.5 km.

## METHOD AND RESULTS

### MT Survey

MT data acquisitions are surface-based passive measurements of the natural time variations of the Earth's magnetic and electric fields to determine the electrical subsurface resistivity. The measured time series of the field components are processed to complex frequency dependent quantities and the ratio of electric to magnetic horizontal components is related to an apparent resistivity,

$$\rho_{xy} = \frac{i}{\omega\mu_0} \left| \frac{E_x}{H_y} \right|^2 \quad (1)$$

where  $i$  the imaginary unit,  $\omega$  the angular frequency and  $\mu_0$  the vacuum permeability.  $E_x$  and  $H_y$  denote, respectively, the orthogonal horizontal electric and magnetic field components, where the x-coordinate is usually pointing to geomagnetic north. In general, the horizontal magnetic field components in both orthogonal directions have associated horizontal electric field components, which is expressed in a tensor relationship for the impedance tensor  $\mathbf{Z}$  (Vozoff, 1991, p. 658),

$$\begin{pmatrix} E_x \\ E_y \end{pmatrix} = \begin{pmatrix} Z_{xx} & Z_{xy} \\ Z_{yx} & Z_{yy} \end{pmatrix} \begin{pmatrix} H_x \\ H_y \end{pmatrix} \quad (2)$$

Analysis of the impedance tensor (and the related phase tensor) can provide valuable insights about dimensionality of underlying geoelectrical structures and whether the data is in some way distorted (e.g. Weaver et al., 2003). In 2D, the impedance tensor simplifies with the two diagonal field components being zero. In this case there are two apparent resistivities defined: parallel and orthogonal to geoelectric strike (e.g., Simpson and Bahr, 2005, p.35), referred to as transverse electric (TE) and transverse magnetic (TM) mode respectively.

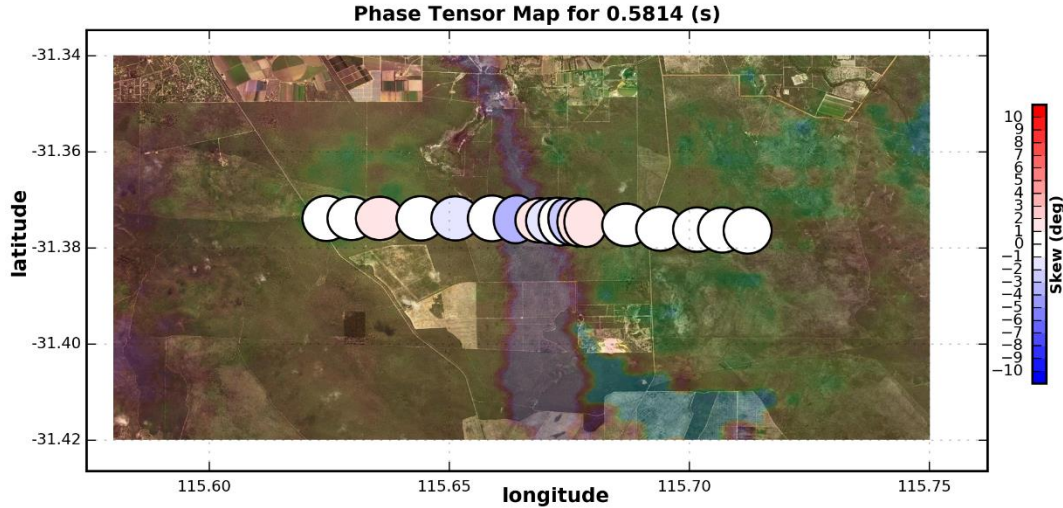


**Figure 3** Plot of phase tensor ellipses for period  $\sim 0.6$  s, coloured according to the value of the ellipses skew angle  $\beta$ . Skew angles  $|\beta| < 4^\circ$  indicate periods where a two-dimensional earth is assumed. Circular ellipses with small value of  $\beta$  indicate 1D structure. The phase tensors ellipses are overlain on a map of the region together with the AEM derived conductivities at a depth of 50 m below the surface. The Badaminna Fault zone is clearly visible as a conductive high anomaly in the centre of the map.

The magnetotelluric data was recorded in single-site mode at a total of 20 sites along a west-east oriented line covering a length of about 10 km approximately perpendicular to the known Badaminna Fault zone. Average site interval was 300-500 m, reducing to 150-180 m for sites located on the fault zone. Magnetotelluric data in AMT as well as MT frequency bands were collected. A GPS synchronised Phoenix v8 system was used for data acquisition, recording two horizontal magnetic and electric channels using non-polarizable porous pots for the electric fields and MTC-50/AMTC-30 coils for the magnetic fields; tipper data was not recorded. The recording time for the AMT data ranged from 2 to 4 hours, while the MT data were recorded twice as long. Robust processing of the raw AMT/MT time-series to frequency dependent impedance tensors was carried out using the proprietary Phoenix processing software. MT and AMT data were merged and stored in EDI format. The EDI files were post-processed and noisy data points removed. Finally, the impedance tensors were rotated based on estimated geo-electrical strike, and the impedance data was converted to apparent resistivity and phase ready for inversion. Phase tensor analysis (Caldwell et al., 2004) shows that the data is mostly 1D/2D with phase tensor skew  $|\beta| < 4^\circ$  (Figure 3). Note that the major axis of most phase tensor ellipses over the fault are aligned parallel to the strike of the conductivity distribution.

The final cleaned data set for input for inversion consisted of a maximum of 72 frequencies between 0.3 Hz and 10 kHz, with signals predominantly in the AMT range. The low frequency part  $< 0.3$  Hz was of low quality, mainly due to the relative short acquisition period at most stations, and was discarded. The skin-depth formula as a rule of thumb for the expected depth range provides a broad estimate from 20 m (10 kHz) to about 4 km (0.3 Hz), based on a simple average resistivity value from nearby borehole logs of 20 ohm-m.

### MT Inversion setup

First results using unconstrained 2D inversions were obtained with well-known Occam2D (deGroot-Hedlin and Constable, 1990) and Mare2DEM (Key and Ovall, 2011); the latter is based on adaptive unstructured meshes and fully MPI parallelised. Both programs use the Occam inversion algorithm, which seeks to find the smoothest model to fit the data within some error tolerance, rather than fitting the data as close as possible where model roughness is maximised (Constable et al., 1987).

Different starting models were trialled, from simple half-space models, to starting models incorporating resistivity values from AEM inversion results, and models including topography, simple bathymetry and the Darling Fault in the east. While all inversion results had overall similar features, starting models incorporating AEM-derived resistivities seemed to give results more compliant with the understanding of the shallow features up to 300 m. The AEM-derived resistivities are based on inversion of Tempest AEM data spanning an area of about 60 km × 40 km. The data has previously been reprocessed where the shallow conductivity distribution was mapped in 3D up to a depth of 300 m (Pethick and Harris, 2016). A cross-section through the AEM resistivity model coinciding with the MT line was used as a starting model for 2D inversion of the MT data, on display in Figure 2 (A).

The figure shows the starting model overlain on a seismic transect coincident with the magnetotelluric survey. The AEM inversion results are displayed in conductivities with units of mS/m. Superimposed are conductivity well logs (from 64'' resistivity logs) on the same colour scale as the AEM. To the west of the Badaminna Fault a significant conductive feature can be seen between ~60 m and ~160 m, identified as the Kardinya Shale, which mainly consists of interbedded siltstones and shales (Davidson, 1995, p. 39). The Wanneroo aquifer underlies the Kardinya Shale, exhibiting an average formation conductivity of ~30 mS/m. On the eastern side of the Badaminna Fault the Wanneroo aquifer is in direct contact with the unconfined Superficial aquifer, as the result of vertical fault displacement. Here, the South Perth Shale Member underlies the Wanneroo aquifer.

Figure 2 (B) provides additional context and shows the onshore Bouguer gravity (Brett, 2017), overlain on a map of the central Perth Basin, clearly showing the Darling Fault anomaly and the low Bouguer values of the sedimentary central Perth Basin. The offshore part of the basin shows the continental shelf, which here extends about 100 km offshore to the edge of continental crust in water depths of up to 4.5 km. The location of the magnetotelluric survey is indicated on the map, which is ~20 km from the Indian Ocean and ~30 km from the Darling Fault, separating the Perth Basin from the granitic Yilgarn Craton. The starting model for the inversion result discussed below included bathymetry and topography 100 km to either side of the MT survey line, the model was further compartmentalized based on the seismic horizons and faults; AEM-derived resistivities were assigned to the shallow part and a constant resistivity value of 100 ohm-m up to 4 km over a resistive half-space of 1000 ohm-m.

### MT Inversion result

Figure 4 shows the inversion result as viewed from the south for the upper 2.5 km along the MT transect after 23 iterations with a final RMS of 2.5. Interpreted seismic horizons together with conductivity well logs on the same linear colour scale are superimposed. In Figure 5 the inversion result is displayed as viewed from the north together with a seismic image crossing the MT transect at an angle. The seismic shows two prominent horizons identified as the Base of the Yarragadee (Cadda Fm) and the Cattamarra Coal Measures together with a conductivity well log from petroleum well Badaminna-1, about 4 km north from the survey site (c.f. Crostella and Backhouse, 2000, p. 32). The well log shows how at depth the conductivity increases in the Cattamarra Coal Measures, consistent with the MT inversion result. The MT recovered conductivity model shows a general agreement in resistivity trends at the well locations. An overall west-east resistivity division due to the Badaminna fault is evident. Furthermore several features corresponding to known geological formations stand out in the image and are identified in Table 1.

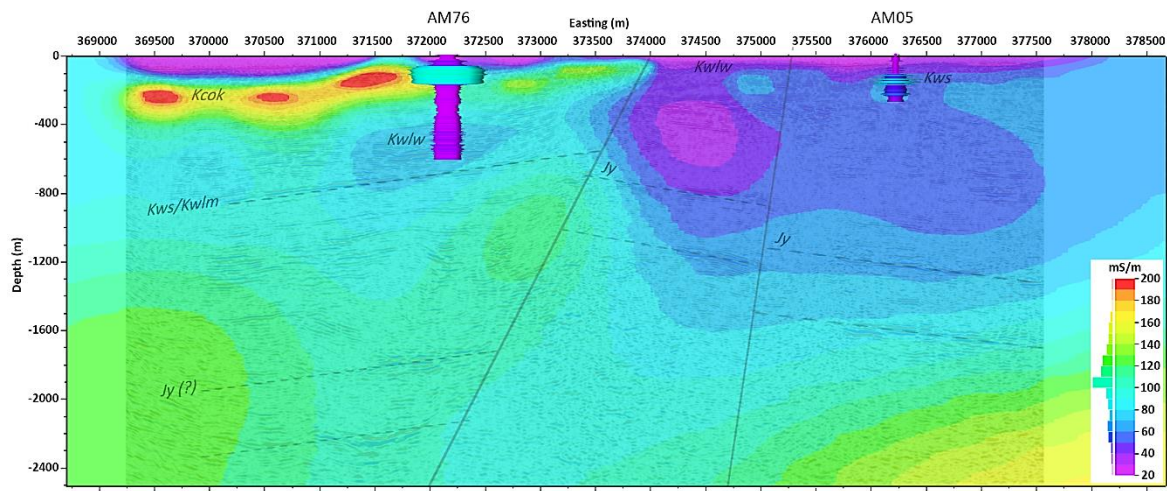
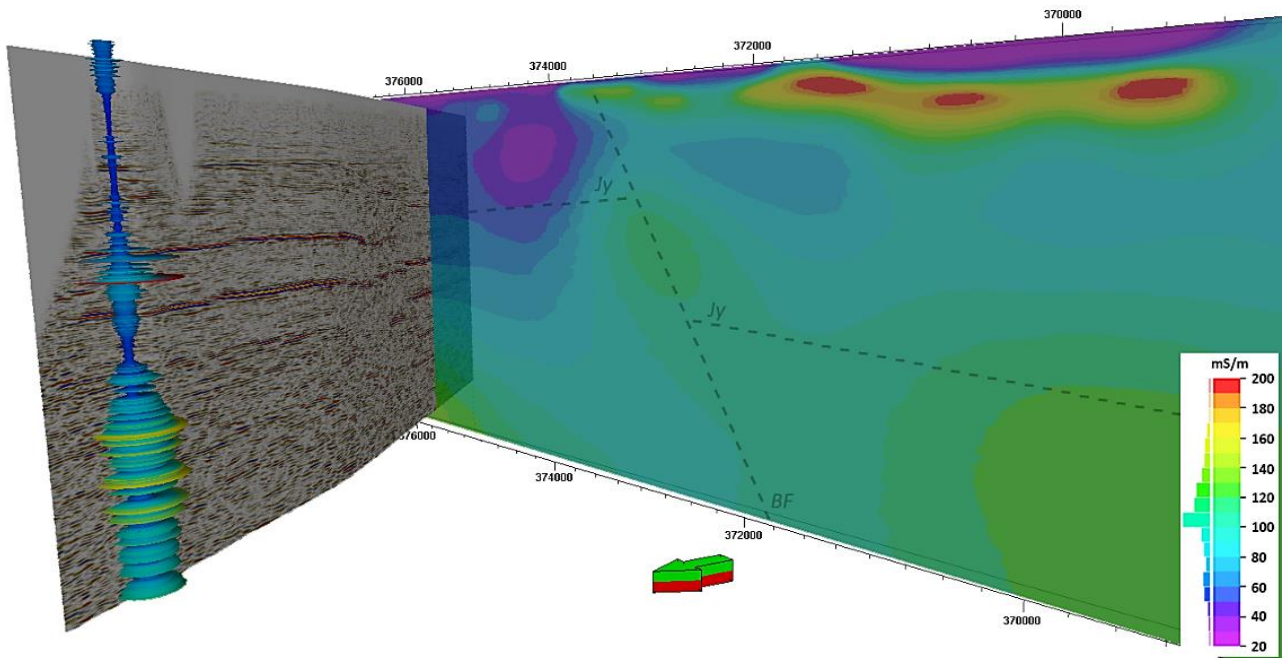


Figure 4 The MT inversion result after 23 iterations shown as conductivities in mS/m overlain on the collocated seismic transect together with interpreted seismic horizons (see Figure 2 for description of hydrostratigraphy). Also shown are well logs from monitoring wells AM76 (west) and AM05 (east) in mS/m. The west-east division of the Badaminna Fault is apparent in the conductivity model with main features further identified in the table below (vertical exaggeration 1.2).

**Table 1 Main features identified in the inversion result**

West	East
<p>The near surface shows the high resistive zone of the here mainly sandy Superficial formations (Davidson, 1995, p. 43).</p> <p>Below the Superficial the Kardinya Shale is prominently noticeable with high conductivities at &gt; 150 mS/m.</p> <p>The Wanneroo aquifer appears underneath from about 300–600 m as a more resistive region. This follows the trend seen in the conductivity log from monitoring well AM76 (however MT derived conductivities are about a factor 2 different).</p> <p>At larger depths, the results are more smeared due to the diffusive nature of the MT method. An oval-shaped conductive zone can be seen below the Wanneroo, probably related to shaly units Mariginiup and South Perth Shale.</p> <p>The broad conductive feature at the western edge may be indicative of the underlying Cattamarra Coal Measures in which the connate waters exhibit high salinities in the survey area (Crostella and Backhouse, 2000, p. 33).</p>	<p>Like ‘West’, the top shows the Superficial Fm.</p> <p>The South Perth Shale can be recognized underneath, showing zones of somewhat elevated conductivities.</p> <p>The Wanneroo aquifer here overlies the South Perth Shale at relative shallow depth in connection with the Superficial. Conductivity values are broadly corresponding to the log from monitoring well AM05.</p> <p>The Yarragadee aquifer underlies the South Perth Shale and can here be identified by the relative high resistivity anomaly.</p> <p>Underneath the resistive high zone of the Yarragadee, the conductivity increases corresponding to horizons seen in seismic imaging, which are presumably the Cadda and Cattamarra Coal Formations. As in the western part, conductivity values increase at depth due to higher salinities.</p> <p>Of interest is the channel-like structure in the centre crossing the Badaminna Fault zone just below the Kardinya Shale, possibly revealing flow paths between the Wanneroo (West) and the Yarragadee (East).</p>



**Figure 5** Inversion result as viewed from the north together with a conductivity well log from petroleum well Badaminna-1, located about 4 km north from the survey site. The well log shows an increasing conductivity in the Cattamarra Coal Measures, which seems overall consistent with the MT inversion result. Also shown is a seismic image crossing the MT transect at an angle, showing two prominent horizons identified as the Base of the Yarragadee (Cadda Fm) and the Cattamarra Coal Measures. The depth scale is from 0 to 2500 m with a vertical exaggeration of 1.2 applied.

## CONCLUSIONS

MT data acquisition in higher frequency bands is less involved than active source EM and has the potential to provide valuable information of hydrogeological interest to depths larger than typical monitoring wells. Here, together with co-located seismic data, the electromagnetic data from AEM and MT form a spatially continuous set of geophysical observations, spanning a large sequence of the upper aquifer systems along the MT transect from the surface to depths larger than 2 km. Resistivity logs from monitoring wells provide crucial interpretive context for the electromagnetic data within overlapping regions and served to 'ground-truth' the inversion results.

Various Occam-style inversions of magnetotelluric data across a basin-scale fault zone were trialled using successively more complex starting models, from simple half-space models to more geologically representative models. Including shallow AEM-derived starting resistivities resulted in relatively better resolved models congruent with borehole information at two locations, west and east of the Badaminna Fault zone. The unconstrained inversion result was able to characterise hydrostratigraphic units offset by vertical fault displacement. Recovered resistivities are broadly consistent with known geology, and possibly suggesting a zone of potential fluid pathways across the fault connecting the Wanneroo and Yarragadee aquifers. Resolution at larger depths deteriorates as is common in diffusive EM methods, however broad conductive structures at increasing depth can be linked to increasing salinities, which are known to increase in the survey region within the Cattamarra Coal Measures.

## REFERENCES:

- Barron, O., Froend, R., Hodgson, G., Ali, R., Dawes, W., Davies, P., and D. McFarlane, 2014, Projected risks to groundwater-dependent terrestrial vegetation caused by changing climate and groundwater abstraction in the Central Perth Basin, Western Australia, *Hydrological Processes*, 28, 5513-5529, DOI: 10.1002/hyp.10014
- Brett, J.W., 2017, 400 m gravity merged grid of Western Australia 2017 version 1, Geological Survey of Western Australia, Perth
- Constable, S.C., Parker R.L. and C.G. Constable, 1987, Occam's inversion: A practical algorithm for generating smooth models from electromagnetic sounding data, *Geophysics*, 52, 289-300
- Crostella, A., and J. Backhouse, 2000, Geology and petroleum exploration of the central and southern Perth Basin, Western Australia, *Western Australia Geological Survey, Report 57*, 85p.
- Caldwell, T.G., Bibby, H.M. and C. Brown, 2004, The magnetotelluric phase tensor, *Geophysical Journal International*, 158, 457-469
- DoW, 2016 (in preparation), Perth region aquifer re-conceptualisation report, Government of Western Australia, Department of Water, *Hydrogeological Record Series, Report no. HR 363*
- DoW, 2017, Environmental management of groundwater from the Gngangara Mound, Government of Western Australia, Department of Water, *Annual compliance report*
- deGroot-Hedlin, C., and S. Constable, 1990, Occam's inversion to generate smooth two-dimensional models from magnetotelluric data, *Geophysics*, 55, 1613-1624
- Davidson W.A., 1995, Hydrogeology and groundwater resources of the Perth region Western Australia, *Geological Survey of Western Australia, Bulletin 142*
- Key, K., and J. Oval, 2011, A parallel goal-oriented adaptive finite element method for 2.5-D electromagnetic modelling, *Geophysical Journal International*, 186, 137-154, doi:10.1111/j.1365-246X.2011.05025.x
- Leyland, L.A., 2012, Reinterpretation of the hydrogeology of the Leederville aquifer: Gngangara groundwater system, Government of Western Australia, Department of Water, *Hydrogeological record series, Report no. HG 59*.
- Pethick, A., and B. Harris, 2016, Macro-parallelisation for controlled source electromagnetic applications, *Journal of Applied Geophysics*, 124, p. 91-105.
- Simpson, F. and K. Bahr, 2005, *Practical magnetotellurics*, Cambridge University Press
- Vozoff, K., 1991, The magnetotelluric method, In Nabighian, M.N. (ed.), *Electromagnetic Methods in Applied Geophysics*. Tulsa, OK: Society of Exploration Geophysicists, pp. 641-712.
- Weaver, J.T., Agarwal, A.K. and F.E.M. Lilley, 2006, The relationship between the magnetotelluric tensor invariants and the phase tensor of Caldwell, Bibby, and Brown, *Exploration Geophysics*, 37, 261-267
- Water Corporation, 2016, *Annual Report*